ISSN 0020-1685, Inorganic Materials, 2011, Vol. 47, No. 6, pp. 583–587. © Pleiades Publishing, Ltd., 2011.
Original Russian Text © D.M. Babanly, 2011, published in Neorganicheskie Materialy, 2011, Vol. 47, No. 6, pp. 658–661.

Composition Range and Thermodynamic Properties of Tl_5Se_2Br-Based Solid Solutions

D. M. Babanly

Institute of Chemical Problems, Academy of Sciences of Azerbaijan, pr. Javida 29, Baku, AZ1143 Azerbaijan
e-mail: Babanly_mb@rambler.ru

Received March 31, 2010

Abstract—The equilibrium subsolidus phase diagram of the TlBr–Tl_2Se–TlSe system has been mapped out using X-ray diffraction analysis and emf measurements on thallium concentration cells. Tl_5Se_2Br has been shown to have a broad homogeneity region. The emf results are used to evaluate the relative partial thermodynamic functions of the thallium in the alloys studied and the standard integral thermodynamic functions (ΔG^0(298 K), ΔH^0(298 K), S^0(298 K)) of the Tl_5Se_2Br-based solid solutions.

DOI: 10.1134/S002016851106001X

INTRODUCTION

Knowledge of phase equilibria and thermodynamic properties of phases is of key importance in designing techniques and optimizing conditions for the fabrication of multicomponent inorganic materials.

Metal chalcogenides, in particular, thallium chalcogenides, and related phases are of interest for the development of advanced semiconducting, thermoelectric, and other functional materials.

The ternary system Tl–Se–Br has been studied in detail in the composition region Tl–TlBr–Se [1–6]. Blachnic and Dreisbach [1] investigated the pseudobinary join TlBr–Tl_2Se and identified a compound of compositionTl_5Se_2Br, melting congruently at 745 K. Tl_2Se was shown to dissolve up to ~20 mol % TlBr at 650 K.

Tl_5Se_2Br has a tetragonal structure (Tl_5Te_3 type, sp. gr. $I4/mcm$) with lattice parameters $a = 8.594$ Å and $b = 12.788$ Å ($Z = 4$) [2] and forms a eutectic with TlSe [3].

According to Peresh et al. [4], the TlBr–TlSe system is also pseudobinary and has a simple binary eutectic. At the same type, a later study [5] revealed a monotectic equilibrium in this system.

Babanly et al. [6] constructed the T–x–y phase diagram of the Tl–Se–Br system in the Tl–TlBr–Se composition region, a number of vertical sections, and the 400-K isothermal section of the phase diagram and identified primary crystallization fields and the types and coordinates of invariant equilibria. The homogeneity region of Tl_5Se_2Br was shown to extend well beyond the pseudobinary join TlBr–Tl_2Se toward the selenium corner.

The purpose of this work was to accurately determine the homogeneity region of Tl_5Se_2Br and to study the thermodynamic properties of Tl_5Se_2Br-based solid solutions.

EXPERIMENTAL

We used earlier data [6] to optimize sample compositions for studies of the TlBr–Tl_2Se–TlSe system by X-ray diffraction (XRD) analysis (DRON-2 diffractometer, CuK_α radiation) and emf measurements and select synthesis and heat-treatment conditions.

Tl_2Se and TlSe were synthesized by a sealed-ampule technique: high-purity components (TL-000 thallium and OSCh 17-3 selenium) were reacted at 700–750 K in ampules pumped down to ~10^{-2} Pa. TlBr was synthesized as described elsewhere [7]. Metallic thallium was dissolved in dilute (5%) H_2SO_4 at ~350 K. Dilute HBr was added to a boiling 2% Tl_2SO_4 solution until complete precipitation occurred. After cooling, TlBr was separated from the mother liquor, washed with distilled water, and dried for a long time in a drying oven at 110–120°C. Since TlBr is difficult to recrystallize, the residual mother liquor was removed by multiple boiling with water, followed by suction filtration. The product was dried in a desiccator over KOH at 390–400 K and stored in the dark to avoid photodecomposition.

The synthesized compounds were identified by differential thermal analysis and X-ray diffraction. TlBr–Tl_2Se–TlSe samples were prepared by melting appropriate mixtures of the binary compounds and elemental selenium in evacuated silica ampules. The alloy compositions chosen lay on the lines connecting TlSe with the Tl_5Se_2Br–Tl_5Se_3 join at 20, 40, 60, and 80 mol % Tl_5Se_2Br. The alloys were annealed at 650 K for 300 h, at 550 K for 1000 h, and finally at 400 K for 300 h.

In emf measurements, we used concentration cells of the type

$$(-)\ \mathrm{Tl}\ (s)\ |\ \text{liquid electrolyte, } \mathrm{Tl}^+\ |\ (\mathrm{TlBr{-}Tl_2Se{-}TlSe})\ (s)\ (+), \qquad \text{(I)}$$

with electrodes of pure metallic thallium (left-hand electrode) and equilibrated TlBr–Tl_2Se–TlSe alloys (right-hand electrode).

The left-hand electrode was made by attaching metallic thallium (99.99+% purity) to a molybdenum current lead. Given that thallium and the alloys under consideration readily oxidize in air even at room temperature, before assembling the cell the electrodes were stored in glycerol, which is nonreactive with metallic thallium [8].

The right-hand electrode was fabricated by pressing powder of an equilibrated alloy onto a current lead in the form of a cylindrical pellet ~8 mm in diameter and 3–5 mm in thickness.

The electrolyte used was a glycerol solution of KBr with TlBr additions. Given that the electrolyte must be free of moisture and oxygen, the glycerol (analytical grade) was thoroughly dried and degassed at ~400 K under dynamic vacuum, and reagent-grade KBr and TlBr were used.

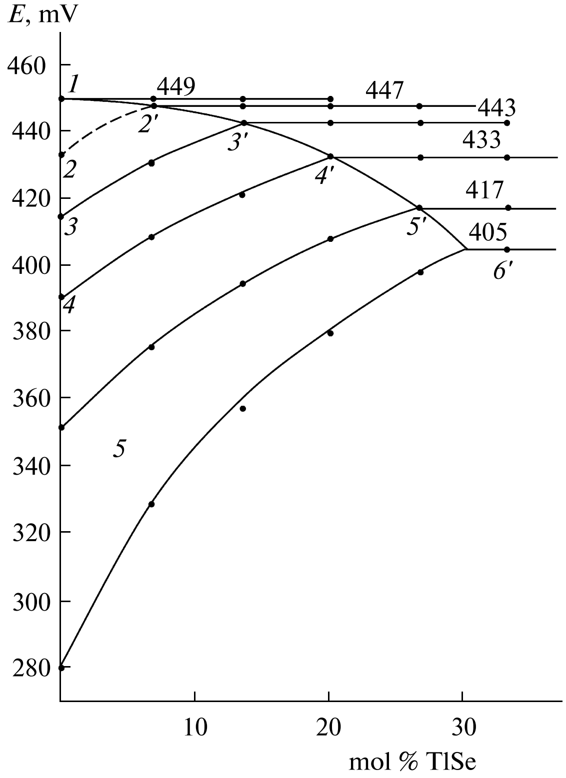

Fig. 1. Composition dependences of the 300-K emf of concentration cells of the type (I) for Tl_2Se–TlSe–Tl_5Se_2Br alloys; (*1–6; 2'–6'*) see text.

The procedures utilized to set up electrochemical cells and measure their emf are described in detail elsewhere [6, 9]. The emf was measured from 300 to 430 K by a compensation technique using a V-7-27 digital voltmeter. The equilibrium emf was first measured 40–60 h after the cell had been held at 380 K; subsequently, measurements were taken every 3–4 h after the temperature had stabilized. Equilibrium was thought to be reached when emf values obtained in repeated measurements at a given temperature differed by no more than 0.5 mV, independent of whether the temperature was raised or lowered.

RESULTS AND DISCUSSION

Figure 1 shows the composition dependences of the 300-K emf for Tl_2Se–Tl_5Se_3–Tl_5Se_2Br alloys with compositions along lines issuing from the Tl_2Se corner. The alloy compositions in one of the constituent binaries are given by $(0.333\mathrm{TlBr} \cdot 0.667\mathrm{Tl_2Se})_{1-x}(\mathrm{Tl_2Se})_x$ with $x = 0$, 0.14, 0.31, 0.50, 0.73, and 1 (*1–6*).

The emf of alloy *6* (pure Tl_2Se) differs very little from that reported by Vasil'ev et al. [10], and those of alloys *1 –5* are in excellent agreement with data presented in Babanly et al. [6] (Fig. 2).

All the other alloys were prepared by adding TlSe to alloys *1–6*. As seen in Fig. 1, the emf of alloy *1* (Tl_5Se_2Br) is 449 mV and remains unchanged on the addition of TlSe. A different picture is observed for alloys *2–5*: with increasing TlSe content, the emf increases until points *2'–5'* are reached and then remains constant, independent of the overall composition. The $(\mathrm{Tl_5Se_2Br})_{1-y}(\mathrm{Tl_5Se_3})_y$ alloy compositions with $y = 0$, 0.2, 0.4, 0.6, and 0.8 at points *2'–5'* lie on the Tl_5Se_3–Tl_5Se_2Br join.

Thus, the present emf data indicate that the Se-rich phase boundary of the Tl_5Se_2Br (δ) and Tl_2Se-based (α) solid solutions almost coincides with the Tl_5Se_3–Tl_5Se_2Br join. Note also that, in the constituent binary system Tl_2Se–TlSe, the emf is a continuous function of composition in the range 0–30 mol % TlSe. Tl_5Se_3 (alloy *6'*) lies beyond the homogeneity region of the (Tl_2Se-based) α-phase (Fig. 1), in accordance with the phase diagram of the Tl–Se system [11] and data reported by Vasil'ev et al. [10].

The above data, in conjunction with XRD results, were used to construct the subsolidus phase diagram of the Tl_2Se–TlSe–Tl_5Se_2Br system (Fig. 2). As seen in Fig. 2, the homogeneity regions of the α- and δ-phases extend well beyond the pseudobinary system Tl_2Se–Tl_5Se_2Br, into the Tl_2Se–TlSe–Tl_5Se_2Br

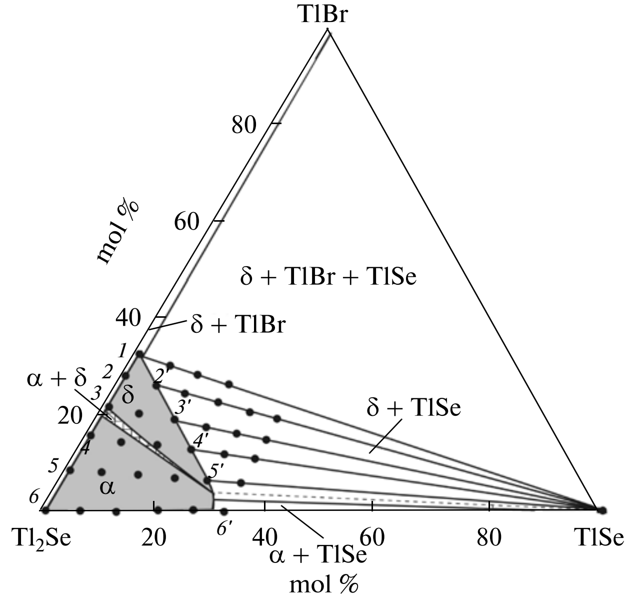

Fig. 2. Subsolidus phase diagram of the Tl_2Se–TlSe–TlBr system; the points represent the alloy compositions studied; (*1–6; 2'–6'*) see text.

composition triangle, reaching the Tl_5Se_2Br–Tl_5Se_3 join. As a result, the homogeneity region of the δ-phase considerably broadens, whereas the α + δ two-phase region narrows down, transforming into an α ⟷ δ morphotropic phase boundary. XRD characterization of thoroughly homogenized alloys *2'–5'* showed that their XRD patterns were very similar to that of Tl_5Se_2Br (Fig. 3).

To assess the thermodynamic properties of the δ-phase along the Tl_5Se_2Br–Tl_5Se_3 join, the emf data for alloys *2'–5'* were represented by least squares linear equations [12] of the form [13] (Table 1)

$$E = a + bT + t\left[\frac{S_E^2}{n} + S_b^2\left(T - \overline{T}\right)^2\right]^{1/2},$$

where S_b^2 is the variance of b, S_E^2 is the variance of an individual emf measurement, n is the number of data points (E and T), $\overline{T}$ is the average temperature, and t is Student's t. For $n \geq 20$ (this study) and a 95% confidence interval, we have $t \approx 2$.

In addition, Table 1 gives the equations derived earlier [6, 14] for the temperature-dependent emf of the Tl_5Se_3 and Tl_5Se_2Br alloys. From the data in Table 1, using well-known thermodynamic relations [9] we evaluated relative partial molar thermodynamic functions of the thallium in the alloys at 298 K (Table 2).

Figure 4 demonstrates that the partial thermodynamic properties of thallium in the Tl_5Se_2Br–Tl_5Se_3 system are continuous functions of composition. In particular, the structure-sensitive function $\Delta\overline{S}(Tl)$ is monotonic in the composition range 0–80 mol % Tl_5Se_3, which indicates, together with the XRD data in Fig. 3, that the structure of the alloys undergoes no qualitative changes.

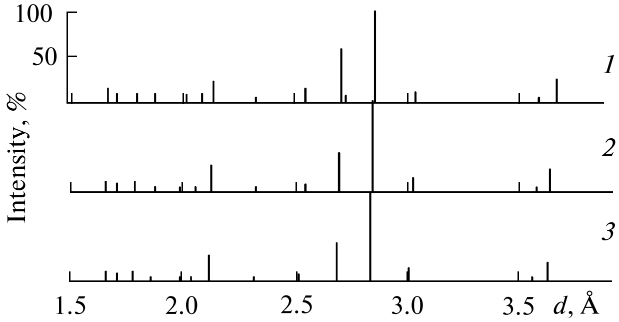

Fig. 3. Schematic XRD patterns of (*1*) Tl_5Se_2Br, (*2*) $Tl_5Se_{2.4}Br_{0.6}$, and (*3*) $Tl_5Se_{2.8}Br_{0.2}$.

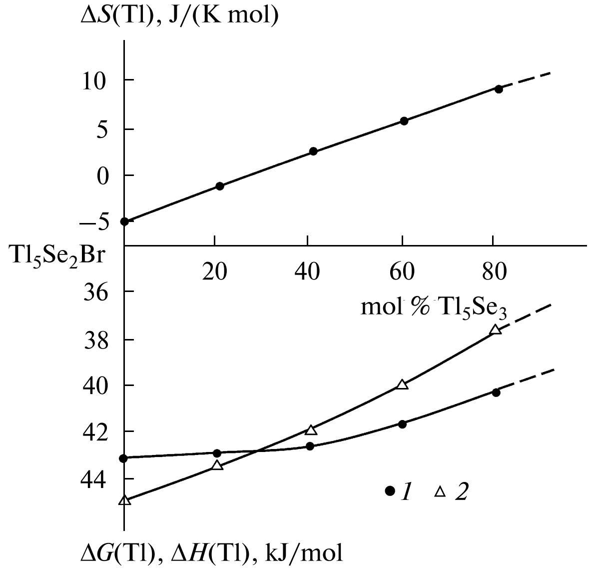

Fig. 4. Composition dependences of the 298-K partial thermodynamic functions of thallium in the Tl_5Se_2Br–Tl_5Se_3 system: (*1*) $\Delta\overline{G}(Tl)$, (*2*) $\Delta\overline{H}(Tl)$.

The integral thermodynamic functions of the $(Tl_5Se_2Br)_{1-y}(Tl_5Se_3)_y$ solid solutions were evaluated by integrating the Gibbs–Duhem equation as described elsewhere [9, 15]. In addition to the data in Table 2, we used the standard thermodynamic functions of formation and standard entropies of TlSe [10, 16] and Tl_5Se_2Br [6] (Table 3). Uncertainties were evaluated by the error propagation method.

It follows from Table 3 that the standard heat and Gibbs energy of the $(Tl_5Se_2Br)_{1-y}(Tl_5Se_3)_y$ solid solutions decrease considerably with decreasing bromine content. The likely reason for this is that the energy of

Table 1. Temperature-dependent emf of cells of the type (I) for $(Tl_5Se_2Br)_{1-y}(Tl_5Se_3)_y$ alloys

Composition	E, mV $= a + bT \pm 2S_E(T)$
Tl_5Se_2Br [6]	$464.7 - 0.053T \pm 2\,[0.93/22 + 3 \times 10^{-5}\,(T - 362.8)^2]^{1/2}$
$Tl_5Se_{2.2}Br_{0.8}$	$449.6 - 0.008T \pm 2\,[1.1/22 + 3.6 \times 10^{-5}\,(T - 361.7)^2]^{1/2}$
$Tl_5Se_{2.4}Br_{0.6}$	$434.1 + 0.028T \pm 2\,[1.6/22 + 5.2 \times 10^{-5}\,(T - 361.7)^2]^{1/2}$
$Tl_5Se_{2.6}Br_{0.4}$	$414.5 + 0.062T \pm 2\,[1.2/22 + 3.2 \times 10^{-5}\,(T - 361.7)^2]^{1/2}$
$Tl_5Se_{2.8}Br_{0.2}$	$389.8 + 0.094T \pm 2\,[1.7/22 + 5.4 \times 10^{-5}\,(T - 361.7)^2]^{1/2}$
Tl_5Se_3 [14]	$368.2 + 0.124T \pm 2\,[1.5/24 + 5 \times 10^{-5}\,(T - 360.6)^2]^{1/2}$

Table 2. Partial thermodynamic functions of the thallium in $(Tl_5Se_2Br)_{1-y}(Tl_5Se_3)_y$ alloys at 298 K

Composition	$-\Delta\overline{G}$(Tl)	$-\Delta\overline{H}$(Tl)	$\Delta\overline{S}$(Tl)
	kJ/mol		J/(K mol)
Tl_5Se_2Br [6]	43.32 ± 0.06	44.84 ± 0.19	−5.11 ± 1.06
$Tl_5Se_{2.2}Br_{0.8}$	43.15 ± 0.09	43.38 ± 0.22	−0.77 ± 1.16
$Tl_5Se_{2.4}Br_{0.6}$	42.69 ± 0.10	41.88 ± 0.23	2.70 ± 1.39
$Tl_5Se_{2.6}Br_{0.4}$	41.78 ± 0.08	39.99 ± 0.21	5.98 ± 1.09
$Tl_5Se_{2.8}Br_{0.2}$	40.31 ± 0.10	37.61 ± 0.24	9.07 ± 1.42
Tl_5Se_3 [14]	39.09 ± 0.09	35.53 ± 0.22	11.96 ± 1.36

Table 3. Standard integral thermodynamic functions of $(Tl_5Se_2Br)_{1-y}(Tl_5Se_3)_y$ solid solutions

Composition	$-\Delta G^0$(298 K)	$-\Delta H^0$(298 K)	S^0(298 K)
	kJ/mol		J/(K mol)
TlSe	60.1 ± 0.1 [10]	61.0 ± 0.5 [10]	102.9 ± 1.7 [16]
Tl_5Se_2Br [6]	374.3 ± 1.0	384.3 ± 2.7	447.6 ± 6.4
$Tl_5Se_{2.2}Br_{0.8}$	360.5 ± 1.1	358.4 ± 2.8	450.4 ± 6.9
$Tl_5Se_{2.4}Br_{0.6}$	340.8 ± 1.1	338.6 ± 2.8	453.3 ± 7.2
$Tl_5Se_{2.6}Br_{0.4}$	317.4 ± 1.2	314.8 ± 2.9	455.5 ± 7.6
$Tl_5Se_{2.8}Br_{0.2}$	288.1 ± 1.3	284.3 ± 3.0	458 ± 8.0

the predominantly ionic Tl–Br bond significantly exceeds that of the Tl–Se bond, which has an ionic–covalent–metallic character.

REFERENCES

1. Blachnik, R. and Dreisbach, H.A., Phase Relations in the TlX–Tl_2Se Systems (X = Cl, Br, I) and the Crystal Structure of Tl_5Se_2I, J. Solid. State Chem., 1984, vol. 52, no. 1, pp. 53–60.
2. Doert, Th., Asmuth, R., and Bottcher, P., Syntheses and Crystal Structures of Tl_5Se_2Cl and Tl_5Se_2Br, *J. Alloys. Compd.*, 1994, vol. 209, pp. 151–157.
3. Babanly, D.M., Jafarova, Z.G., and Yusibov, Yu.A., Phase Equilibria in the Tl_5Se_2Cl(Br)–Tl(TlSe) Systems, *Vestn. Bakinsk. Gos. Univ., Ser. Estestv. Nauk*, 2006, no. 1, pp. 52–55.
4. Peresh, E.Yu., Lazarev, V.B., Kornichuk, O.I., et al., Phase Equilibria in the Tl_2S(Se, Te)–TlI and TlSe–TlCl(Br,I) Systems, *Neorg. Mater.*, 1993, vol. 29, no. 3, pp. 406–410 [*Inorg. Mater.* (Engl. Transl.), vol. 29, no. 3, pp. 334–337].
5. Babanly, D.M., Guseinov, G.M., Yusibov, Yu.A., and Sadygov, F.M., Systems TlBr–TlS(TlSe, TlTe), *IX Respublikanskaya nauchnaya konferentsiya po fiziko-khimicheskomu analizu i neorganicheskomu materialovedeniyu* (IX Azeri Conf. on Physicochemical Analysis and Inorganic Materials Research), Baku, 2004, pp. 108–111.
6. Babanly, D.M., Yusibov, Yu.A., and Babanly, M.B., Phase Diagram and Thermodynamic Properties of the Tl–TlBr–Se System, *Zh. Neorg. Khim.*, 2007, vol. 52, no. 5, pp. 827–833.
7. *Handbuch der präparativen anorganischen Chemie*, von Brauer, G., Ed., Stuttgart: Ferdinand Enke, 1978. Translated under the title *Rukovodstvo po neorganicheskomu sintezu,* Moscow: Mir, 1985, vol. 3, p. 947.
8. Turova, N.Ya. and Novoselova, A.V., Alcohol Derivatives of Alkali Metals, Alkaline-Earth Metals, Magnesium, and Thallium(I), *Usp. Khim.*, 1956, vol. 34, no. 3, pp. 385–433.
9. Babanly, M.B., Yusibov, Yu.A., and Abishev, V.T., *Metod EDS v termodinamike slozhnykh poluprovodnikovykh veshchestv* (EMF Measurements in Thermodynamic Studies of Multicomponent Semiconductors), Baku: Bakinsk. Gos. Univ., 1992.
10. Vasil'ev, V.P., Nikol'skaya, A.V., and Gerasimov, Ya.I., Thermodynamic Study of Thallium–Selenium Alloys Using EMF Measurements, *Zh. Neorg. Khim.*, 1971, vol. 45, no. 8, pp. 2061–2063.
11. *Binary Alloy Phase Diagrams*, Massalski, T.B., Ed., Materials Park: ASM International, 1990, 2nd ed.

12. Doerffel, K., *Statistik in der analytischen Chemie*, Leipzig: Grundstoffindustrie, 1990.
13. Kornilov, A.N., Stepina, L.B., and Sokolov, V.A., Recommendations on Compact Representation of Experimental Data in Reports on Thermochemical and Thermodynamic Studies, *Zh. Fiz. Khim.*, 1972, vol. 46, no. 11, pp. 2974–2979.
14. Guseinov, G.M., Babanly, D.M., Sadygov, F.M., and Babanly, M.B., Thermodynamic Properties and Homogeneity Regions of Tl_6SCl_4 and Tl_5Se_2Cl, *Neorg. Mater.*, 2009, vol. 45, no. 2, pp. 165–170 [*Inorg. Mater.* (Engl. Transl.), vol. 45, no. 2, pp. 129–134].
15. Babanly, M.B. and Kuliev, A.A., Thermodynamic Study and Refinement of the Phase Diagrams of Ternary Chalcogenide Systems Using EMF Measurements, in *Matematicheskie zadachi khimicheskoi termodinamiki* (Mathematical Methods in Chemical Thermodynamics), Novosibirsk: Nauka, 1985, pp. 192–201.
16. Kubaschewski, O., Alcock, C.B., and Spencer, P.J., *Materials Thermochemistry*, Oxford: Pergamon, 1993.